

obtained from the iterative solution of Eq. (4) shows that the maximum difference is less than 1% for the parameters shown in Figs 2-4. Equation (16) may be written in dimensional form as

$$N_{xx} = h^3 \{ G_{xy}/b^2 + m^2 \pi^2 E_{xx} / [12a^2(1 - \nu_{xy}^2 E_{yy}/E_{xx})] \} \quad (17)$$

This equation shows that the smallest buckling load is obtained with $m = 1$. It also shows that the shear modulus (G_{xy}) is dominant for long plates and that the other properties become important for short plates.

References

- Timoshenko, S. and Gere, J. M., *Theory of Elastic Stability*, McGraw-Hill, New York, 1961, pp. 361-363.
- Bridget, F. J., Jerome, C. C., and Vosseller, A. B., "Some New Experiments on Buckling of Thin-Wall Construction," *Transactions of the ASME, Applied Mechanics Division*, Vol. 56, 1934, pp. 569-578.
- Lackman, L. M. and Ault, R. M., "Minimum-Weight Analysis of Filamentary Composite Wide Columns," *Journal of Aircraft*, Vol. 5, No. 2, March-April 1968, pp. 184-190.
- "Advanced Composite Wing Structures; Preliminary Analysis and Optimization Methods," Tech. Rept. AC-SM-7843, Aug. 1968, Grumman Aircraft Engineering Corporation.
- Lekhnitski, S. G., *Anisotropic Plates*, 2nd ed., OGIZ, Moscow-Leningrad, 1947; English ed. translated by S. W. Tsai and T. Cheron, Gordon and Breach, London, 1968.

Equilibrium Shape of an Ablating Nose in Laminar Hypersonic Flow

F. D. HAINS*

The Aerospace Corporation, El Segundo, Calif.

DURING re-entry, the nose of a body may change shape as ablation occurs. In a series of experiments with teflon models, Simpkins¹ obtained stable shapes that were independent of the initial shape of the nose. He also developed a simple theory that gave a final shape not in good agreement with his experimental results. This Note presents a new theory for the equilibrium shape associated with a laminar boundary layer. Numerical results from the theory are then compared with some recent experimental shapes obtained in the Aerospace Corp. arc tunnel. A similar study of the equilibrium shape for a wholly turbulent boundary layer was made by Welsh.²

Consider a circular cylinder with a nose that is undergoing ablation and has reached a stable shape. The local rate of surface erosion is assumed to be proportional to q , the local rate of heat transfer into the body surface. For a stable shape, the condition for uniform axial erosion is

$$q/q_0 = \cos \alpha \quad (1)$$

where α is the angle between the normal to the body surface and the body axis, and q_0 is the stagnation point heat transfer.

Simpkins used the local heat transfer expression

$$Nu/(Re)^{1/2} = 0.66 \quad (2)$$

which is applicable only in the vicinity of the stagnation point. The Nusselt number and Reynolds number are, re-

Received December 19, 1969; revision received March 16, 1970. This work was supported by the U.S. Air Force under Contract F04701-69-C-0066.

* Member of the Technical Staff, Aerodynamics and Heat Transfer Department, Aerodynamics and Propulsion Research Laboratory; presently at Bell Aerospace Co., Buffalo, N. Y.

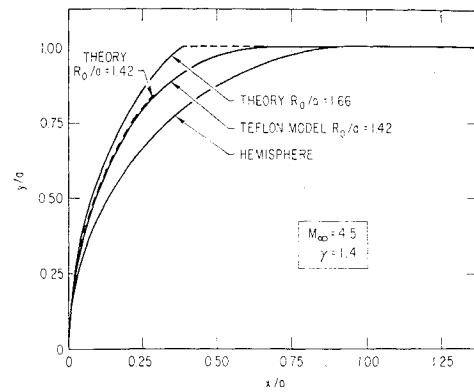


Fig. 1 Comparison of theoretical shapes with experimental shape.

spectively, for unit Prandtl number

$$Nu = qS/\nu_w(H_1 - h_w) \quad (3)$$

$$Re = U_1 S/\nu_w \quad (4)$$

where S is the distance along the body measured from the nose, H_1 and U_1 are the total enthalpy and velocity, respectively, at the outer edge of the boundary layer, and h_w and ν_w are the wall values of enthalpy and kinetic viscosity, respectively. Simpkins approximated the velocity by $U_1 = S(dU_1/dS)_0$, where the derivative is evaluated at the stagnation point. With this assumption, $Re \sim S^2$ and a cancellation with the S in Eq. (3) leaves Eq. (2) independent of a length scale. As a result, Simpkins predicts an equilibrium nose shape whose size is specified by freestream conditions. This is unrealistic because the nose shape should depend on the body scale as well as freestream conditions.

The lack of a body scale was overcome in the present analysis by replacing Eq. (2) with a better estimate of the local heat-transfer rate. The heat-transfer relation for blunt bodies given by Lees³ is

$$q/q_0 = yfT / \left[2 \left(\int_0^S y^2 f ds \right)^{1/2} \right] \quad (5)$$

where

$$f = (p_1/p_0)(U_1/U_\infty) \quad (6)$$

$$T = (U_\infty R_0/\beta_0)^{1/2} \quad (7)$$

Here, p_0 is the stagnation pressure behind the bow shock, U_∞ is the freestream velocity, $\beta_0 = (dU_1/d\alpha)_0$ evaluated at the stagnation point, and R_0 is the nose radius. The quantities p_1 and U_1 are the values of pressure and velocity, respectively, evaluated at the outer edge of the boundary, y is the distance from a point on the body surface to the body axis, and S is the distance to the stagnation point along the body surface.

From the geometry of the body surface

$$ds = dy/\cos \alpha \quad (8)$$

and

$$dx = dy \tan \alpha \quad (9)$$

where x is the coordinate along the centerline of the body. Substituting Eqs. (1) and (8) into Eq. (5), we get

$$\frac{y}{a} = \frac{2 \cos \alpha}{f T^3} \left(\frac{T^2}{R_0} \right) \left(\frac{R_0}{a} \right) \left(\int_0^y \frac{y^2 f}{\cos \alpha} dy \right)^{1/2} \quad (10)$$

which is satisfied by

$$(y/a) = (R_0/a)(T^2/R_0)(f/\cos \alpha) \quad (11)$$

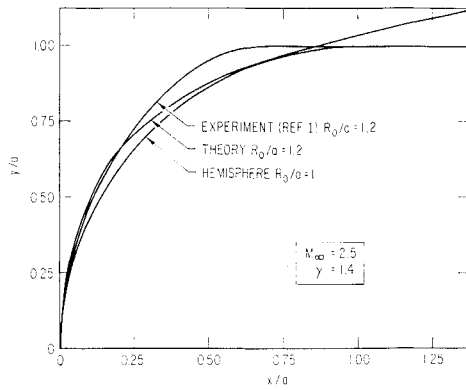


Fig. 2 Comparison of theoretical shape with experimental shape from Ref. 1.

where a is a reference length. For the hemisphere-cylinder considered in this note, a is the radius of the circular cylinder. With the aid of Eq. (11), integration of Eq. (9) yields

$$\frac{x}{a} = \left(\frac{T^2}{R_0}\right) \left(\frac{R_0}{a}\right) \left(\frac{f \tan \alpha}{\cos \alpha} - \int_0^\alpha \frac{f}{\cos^3 \alpha} d\alpha\right) \quad (12)$$

Once the functions f and R_0/T^2 are known, the equilibrium shape can be computed from Eqs. (11) and (12) for particular values of R_0/a . For the shape given in this note, f was computed from Eq. (6) with the Newtonian pressure relation

$$p_1/p_0 = \cos^2 \alpha + (\gamma M_\infty)^{-1} \sin^2 \alpha \quad (13)$$

and the velocity relation

$$u_1/u_\infty = \left\{ \left[\frac{2}{(\gamma - 1)M_\infty^2} + 1 \right] \left[1 - \left(\frac{p_1}{p_\infty} \right)^{(\gamma - 1)/\gamma} \right] \right\}^{1/2} \quad (14)$$

Equation (14) corresponds to isentropic expansion from the stagnation point streamline to the local pressure p_1 . γ is the freestream specific heat ratio, $\tilde{\gamma}$ is the value of γ behind the bow shock, and M_∞ is the freestream Mach number. With the aid of Eqs. (13) and (14), Eq. (7) can be written as

$$R_0/T^2 = \left\{ \left[\frac{2}{(\gamma - 1)M_\infty^2} + 1 \right] \left[\frac{(\tilde{\gamma} - 1)/\tilde{\gamma}}{1 - 1/(\gamma M_\infty^2)} \right] \right\}^{1/2} \quad (15)$$

A comparison of the theoretical shapes obtained from Eqs. (10) and (11) and a typical experimental shape is shown in Fig. 1. Hemisphere-cylinder models with $a = \frac{1}{2}$ in. and overall length of 6 in. were constructed from pure teflon and teflon mixed with 15% graphite. Tests were conducted in the Aerospace Corp. arc tunnel with $M_\infty = 4.5$, $p_0 = 0.2$ atm, and stagnation temperature = 4000°K. Motion pictures of the erosion process revealed that both models approached the same blunted shape, which remained unchanged with further recession. Additional tests with models of different sizes are required to ascertain if this shape is unique.

The theoretical shapes shown in Fig. 1, which are based on the Newtonian pressure formula, terminate at $\alpha = 54^\circ$ because the quantity f in Eq. (11) reaches a maximum. Because further increase in α reduces the values of both x/a and y/a , a branch curve is formed which intersects the y/a axis above the origin. This branch has no physical meaning. The other branch which starts at the stagnation point could probably be continued around the corner if Eq. (1) were modified by the addition of a constant term to the right-hand side, and if Eq. (13) were replaced by a better approximation in the shoulder region.

Two values of R_0/a were used to plot the theoretical shape. Value 1.42 was measured from the models, and the value 1.66 was chosen so that the maximum ordinate of the profile reached the diameter of the cylinder. The former curve fits the experimental shape very well, while the latter is more

blunt. Further experimental investigations will be required to ascertain the generality of $R_0/a = 1.42$ for various size bodies under the same flow conditions.

If the theoretical shape extended to $\alpha = \pi/2$, the value of R_0/a might be determined by the condition $y = a$ at $\alpha = \pi/2$. By raising the pressure over the value given by Eq. (13) when $\alpha > 50^\circ$, it was possible to extend the present analysis to larger values of α , but extension completely around the corner would still require a modification of Eq. (1) because its present form is incorrect as $\alpha \rightarrow \pi/2$.

Figure 2 shows a comparison of the theory with the experimental shape obtained by Simpkins at $M = 2.5$. Value $R_0/a = 1.2$ was measured from a photograph of the model, and the theoretical curve was plotted with the same value of R_0/a . For this lower Mach number, quantity f does not reach a maximum; therefore the curve does not terminate as in Fig. 1. The theory agrees well with the experimental shape near the nose, but deviates from the actual shape in the shoulder region.

References

- ¹ Simpkins, P. G., "On the Stable Shape of Subliming Bodies in a High-Enthalpy Gas," *Journal of Fluid Mechanics*, Vol. 15, No. 1, Jan. 1963, pp. 110-132.
- ² Welsh, W. E., Jr., "Shape and Surface Roughness Effects on Turbulent Nose Tip Ablation," AIAA Paper 69-717, San Francisco, Calif., June 1969.
- ³ Lees, L., "Laminar Heat Transfer over Blunt-Nosed Bodies at Hypersonic Flight Speeds," *Jet Propulsion*, Vol. 26, April 1956, pp. 259-268.

A Shock Wave Attenuation Treatment for Ballistic Ranges

D. HECKMAN,* C. LAHAYE,† L. MOIR,† B. PODESTO,† AND W. ROBERTSON†

Defense Research Establishment Valcartier, Quebec, Canada

AS is well known, the ballistic range consists basically of a long (usually cylindrical) evacuated tank, instrumented at various stations along its length. Projectiles are gun-launched along a path parallel to the axis of the tank and flown past the various instrumented stations. The Defense Research Establishment Valcartier (DREV) has two ballistic range facilities in current operation: Range 3 has a medium size 6-ft-diam tank and Range 5 is a "large" facility,

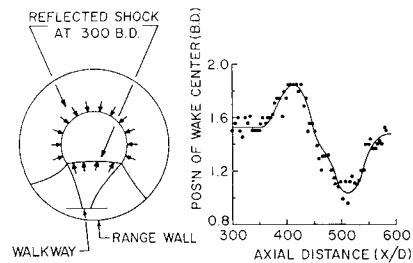


Fig. 1 Wake centerline displacement measured from schlieren movies of a 2.7-in. sphere firing in the asymmetric geometry of Range 5. (Mach number was 13.5 and the ratio of range diameter to sphere diameter was 44.)

Received January 20, 1970; revision received March 6, 1970.
 * Scientific Staff Officer. Member AIAA.
 † Scientific Staff Officer.